Supporting Information

Facet-Dependent Pre-dissolution of Typical Metal Oxide Nanoparticles: Atomic-Scale Mechanisms and Environmental Interfacial Regulation

Shuo Liu[1], Chaofan Deng[1,*], Jinhao Yao[1], Fang Wang[1], Diya A[1], Tongtao Yue[1,*]

[1]*Institute of Coastal Environmental Pollution Control, Key Laboratory of Marine Environment and Ecology, Ministry of Education, Ocean University of China, Qingdao 266100, P.R. China*

[*]Correspondence authors: youknowdcf@stu.ouc.edu.cn (C. Deng), yuetongtao@ouc.edu.cn (T. Yue)

Tables S1–S3: Optimized configurations and adsorption energies of H_2O on ZnO(0001), (11–20), and (10–10) facets for different initial sites and orientations.

Tables S4–S6: Comparison of geometric parameters (bond lengths and angles) before and after H_2O adsorption on the three facets.

Figures S1–S3: Zn–O bond length changes of surface Zn atoms on the three facets upon H_2O adsorption.

Figures S4–S6: Zn–O bond length changes of subsurface and deeper-layer Zn atoms on the nonpolar (11–20) and (10–10) facets upon H_2O adsorption.

Figures S7–S8: Molecular electrostatic potential maps of oxalic acid, phenol, benzoic acid, ethanol, and ammonia.

Table S1. Optimized adsorption configurations and adsorption energies of H_2O on ZnO (0001) for different initial sites and orientations.

Model	Initial structure	Optimized structure	Energy (eV)
	side view	side view	
1	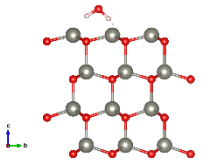	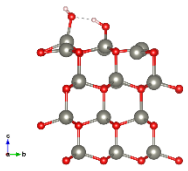	-319.947
2	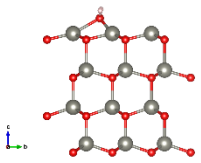	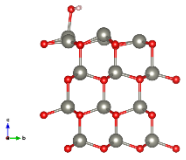	-319.800
3	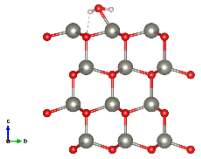	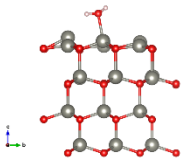	-319.110
4	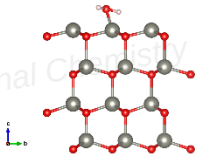	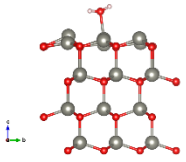	-319.102
5	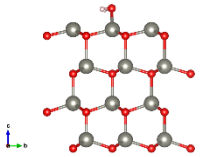	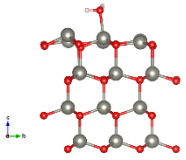	-319.101
6	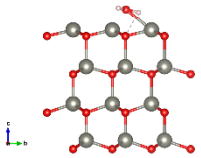	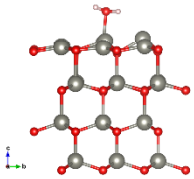	-319.099
7	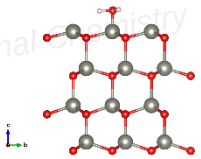	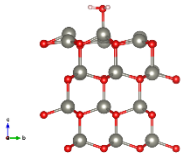	-319.098
8	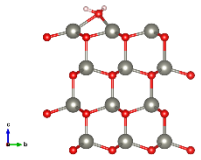	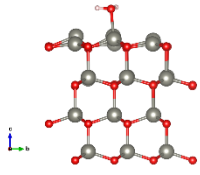	-319.093

Communications in Computational Chemistry

Table S2. Optimized adsorption configurations and adsorption energies of H_2O on ZnO (11–20) for different initial sites and orientations.

Model	Initial structure	Optimized structure	Energy (eV)
	side view	side view	
1	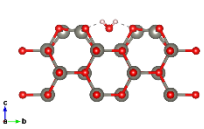	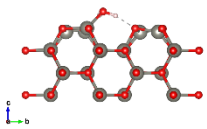	-285.589
2	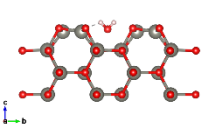	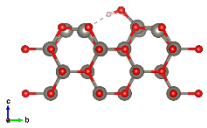	-285.589
3	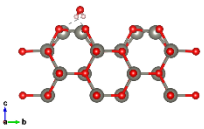	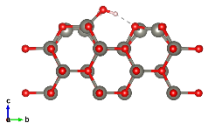	-285.589
4	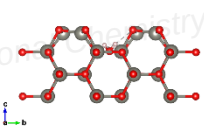	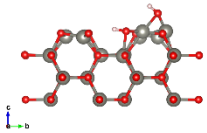	-285.516
5	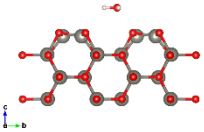	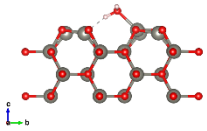	-285.403
6	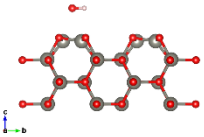	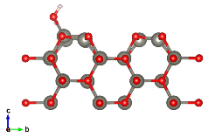	-285.336
7	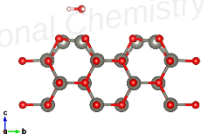	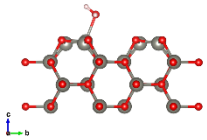	-284.978
8	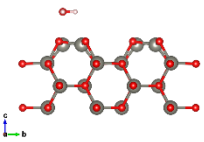	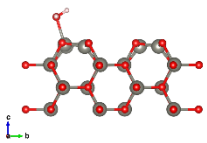	-284.970

Communications in Computational Chemistry

Table S3. Optimized adsorption configurations and adsorption energies of H_2O on ZnO (10–10) for different initial sites and orientations.

Model	Initial structure	Optimized structure	Energy (eV)
	side view	side view	
1	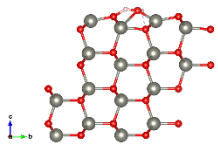	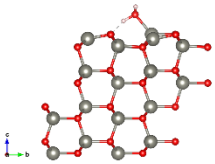	-430.813
2	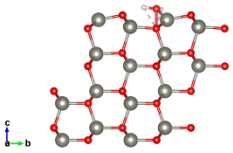	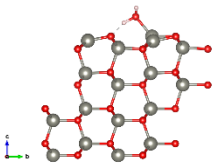	-430.813
3	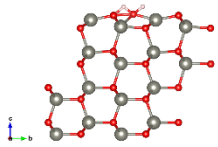	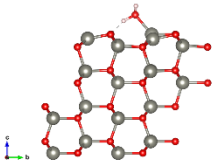	-430.813
4	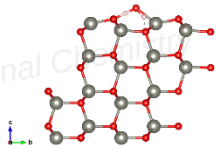	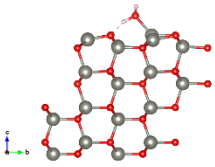	-430.812
5	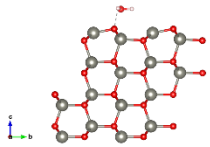	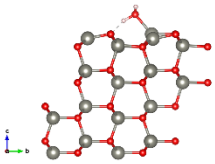	-430.811
6	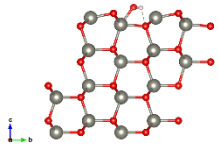	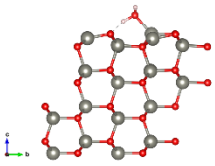	-430.811
7	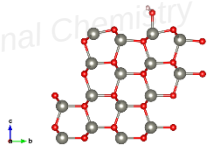	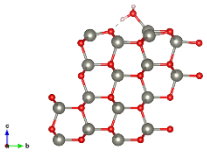	-430.808
8	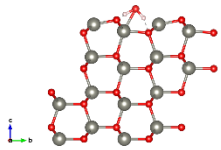	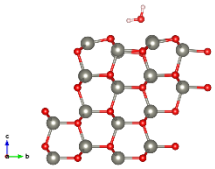	-430.297

Table S4. Geometric parameters associated with water adsorption on the ZnO (0001) facet.

Parameter	Before adsorption	After adsorption
Bond lengths (Å)		
O_w-H_{w1}	**0.97**	**Bond broken**
O_w-H_{w2}	**0.97**	**0.972**
Zn-O_w	**-**	**1.913**
Bond angle (°)		
H_{w1}-O_w-H_{w2}	**104.464**	**Bond broken**

Communications in Computational Chemistry

Table S5. Geometric parameters associated with water adsorption on the ZnO (11–20) facet.

Parameter	Before adsorption	After adsorption
Bond lengths (Å)		
O_w-H_{w1}	**0.97**	**1.005**
O_w-H_{w2}	**0.97**	**1.005**
Zn-O_w	**-**	**2.072**
Bond angle (°)		
H_{w1}-O_w-H_{w2}	**104.464**	**107.266**

Communications in Computational Chemistry

Table S6. Geometric parameters associated with water adsorption on the ZnO (10–10) facet.

Parameter	Before adsorption	After adsorption
Bond lengths (Å)		
O_w-H_{w1}	**0.97**	**0.973**
O_w-H_{w2}	**0.97**	**1.057**
Zn-O_w	**-**	**2.062**
Bond angle (°)		
H_{w1}-O_w-H_{w2}	**104.464**	**108.286**

Communications in Computational Chemistry

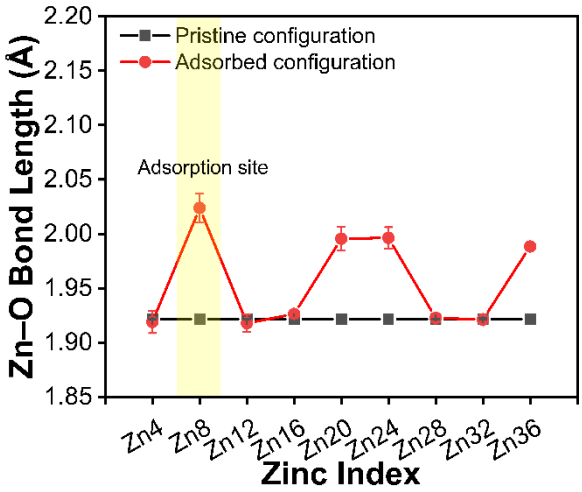

Figure S1. Zn–O bond-length changes of surface Zn atoms on the ZnO (0001) facet before and after water adsorption.

Communications in Computational Chemistry

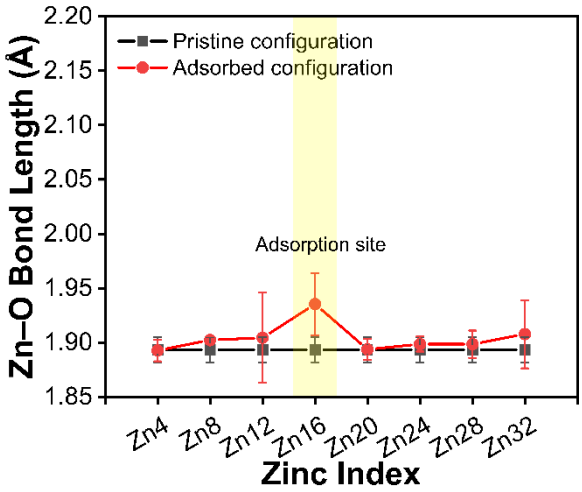

Figure S2. Zn–O bond-length changes of surface Zn atoms on the ZnO (11–20) facet before and after water adsorption.

Communications in Computational Chemistry

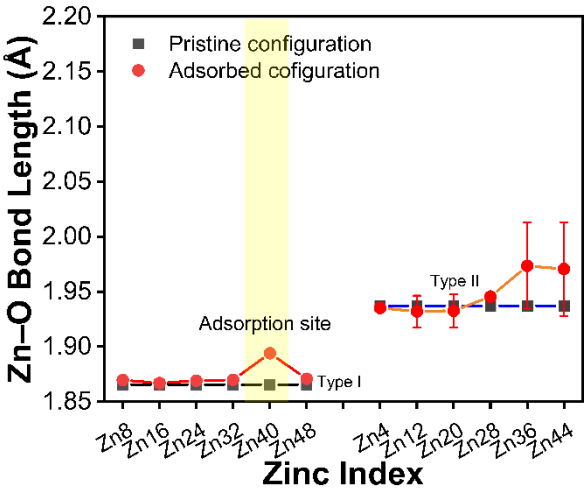

Figure S3. Zn–O bond-length changes of surface Zn atoms on the ZnO (10–10) facet before and after water adsorption. Type I denotes 3-coordinated Zn, and Type II denotes 4-coordinated Zn.

Communications in Computational Chemistry

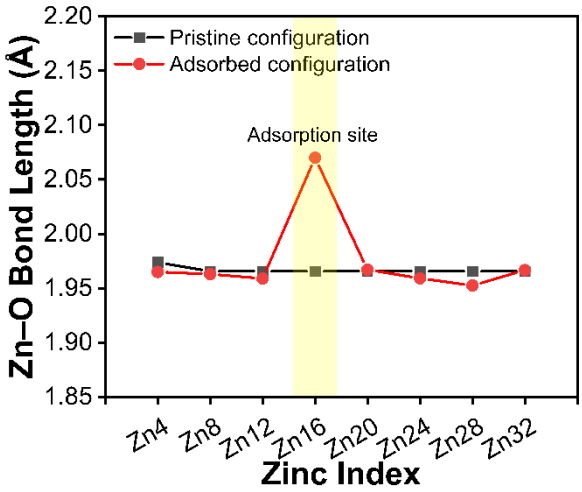

Figure S4. Zn–O bond-length changes of subsurface Zn atoms on the ZnO (11–20) facet before and after water adsorption.

Communications in Computational Chemistry

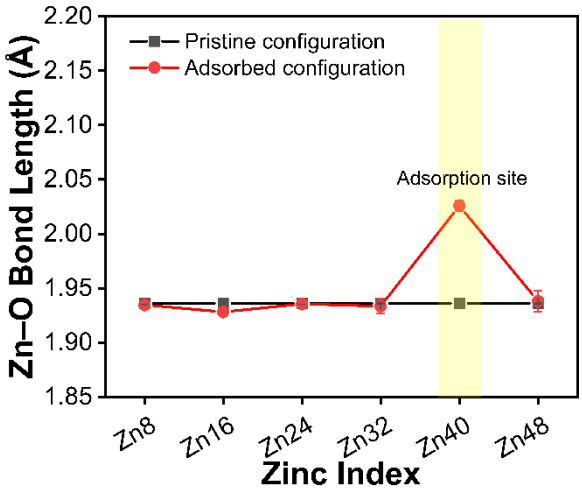

Figure S5. Zn–O bond-length changes of 3-coordinated subsurface Zn atoms on the ZnO (10–10) facet before and after water adsorption.

Communications in Computational Chemistry

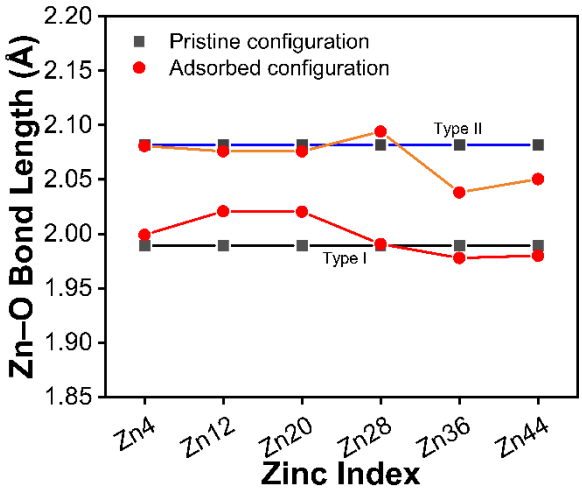

Figure S6. Zn–O bond-length changes of 4-coordinated subsurface and deeper-layer Zn atoms on the ZnO (10–10) facet before and after water adsorption. Type I indicates subsurface Zn, and Type II indicates deeper-layer Zn.

Communications in Computational Chemistry

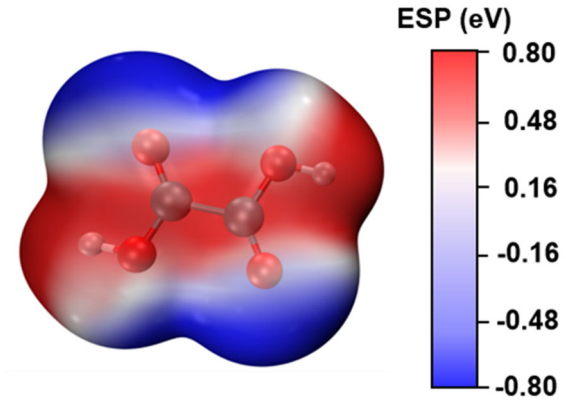

Figure S7. Molecular electrostatic potential map of oxalic acid.

Communications in Computational Chemistry

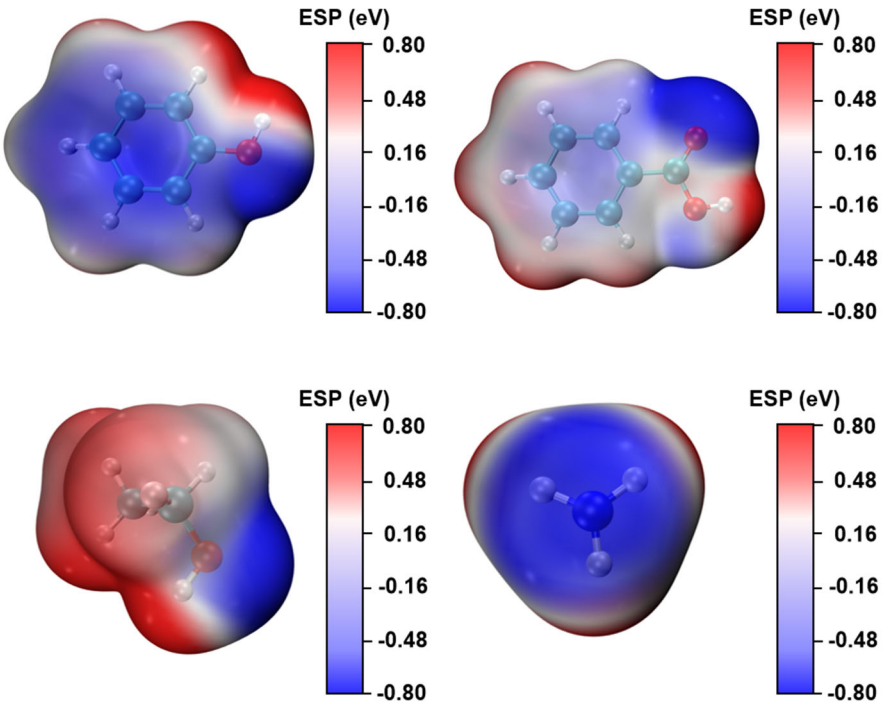

Figure S8. Molecular electrostatic potential maps of phenol, benzoic acid, ethanol, and ammonia.

Communications in Computational Chemistry